NUCLEAR PRECIPITATES IN PYROANTIMONATE-OSMIUM TETROXIDE–FIXED TISSUES

S. S. SPICER, J. H. HARDIN, and W. B. GREENE. From the Institute of Pathobiology and the Department of Pathology, Medical College of South Carolina, Charleston, South Carolina 29401

Recent biochemical studies indicate a significant role for sodium ions in nuclear metabolism. Protein and nucleic acid syntheses in the nucleus depend upon sodium, apparently through a stimulating effect of this cation on the transport of amino acid, purine, and pyrimidine into the nucleus (1). The nuclei of avian erythrocytes and calf thymocytes appear to contain higher sodium concentrations than the cytoplasm (5), and the nuclei of frog oocytes actively incorporate and concentrate sodium as shown by radioautography with Na^{22+} (1).

An ultrastructural method developed by Komnick (8) presumably localizes tissue sodium by precipitating this cation with pyroantimonate (antimonate) ions included in the osmium tetroxide fixative. This method was employed in the present study in an effort to localize the sodium reported to be abundant in the nucleus and to evaluate the possibility of visualizing nucleic acid-linked cations. Use of this technique has yielded results which indicate an abundance of cation, presumably sodium, in the heterochromatin and

nucleoli of several different types of cells. These results were reported in a previous abstract (3).

MATERIALS AND METHODS

Trigeminal ganglia of anesthetized, adult, male, albino rats and cervical lymph nodes of anesthetized, adult, male mice were quickly dissected free and minced into small pieces in chilled fixatives. For ultrastructural study, these tissues were fixed at 4°C by one of three procedures. (*a*) For presumed localization of sodium, specimens were fixed for 1 hr in Komnick's fluid which was modified in the following manner. A 0.1 M (5%) aqueous solution of $K_2H_2 \cdot Sb_2O_7 \cdot 4H_2O$ (potassium pyroantimonate; Fisher Scientific Company, Pittsburgh, Pa.) was prepared by boiling. It was then cooled to room temperature, restored to original volume, and added to an equal volume of a 2% aqueous solution of OsO_4; the pH of this final fixing fluid was adjusted to 7.5 by the addition of acetic acid. (*b*) For controls, specimens were fixed for 1 hr in a solution containing equal volumes of a 0.1 M (3.8%) aqueous solution of $K_4P_2O_7 \cdot 3H_2O$ (potassium pyrophosphate) and a 2% aqueous solution of OsO_4; the pH of this fixative was also adjusted to 7.5 with acid. Unstained thin sections of these control specimens obviously lacked electron-opaque precipitates such as those seen in the specimens fixed with Komnick's fluid. (*c*) A sequence of fixations for 1 hr in cacodylate-buffered 6.25% glutaraldehyde and for 1 hr in collidine-buffered 2% osmium tetroxide was used for ultrastructural study.

After each fixation procedure, the tissue blocks were dehydrated with graded alcohols and infiltrated with and embedded in Maraglas. Ultrathin sections with and without prior staining with lead citrate or uranyl acetate-lead citrate were examined in an AEI-6B electron microscope.

RESULTS

Nuclei with Abundant Heterochromatin

Nuclei of endothelial (Fig. 1), Schwann, and satellite cells and lymphocytes (Fig. 3) fixed with

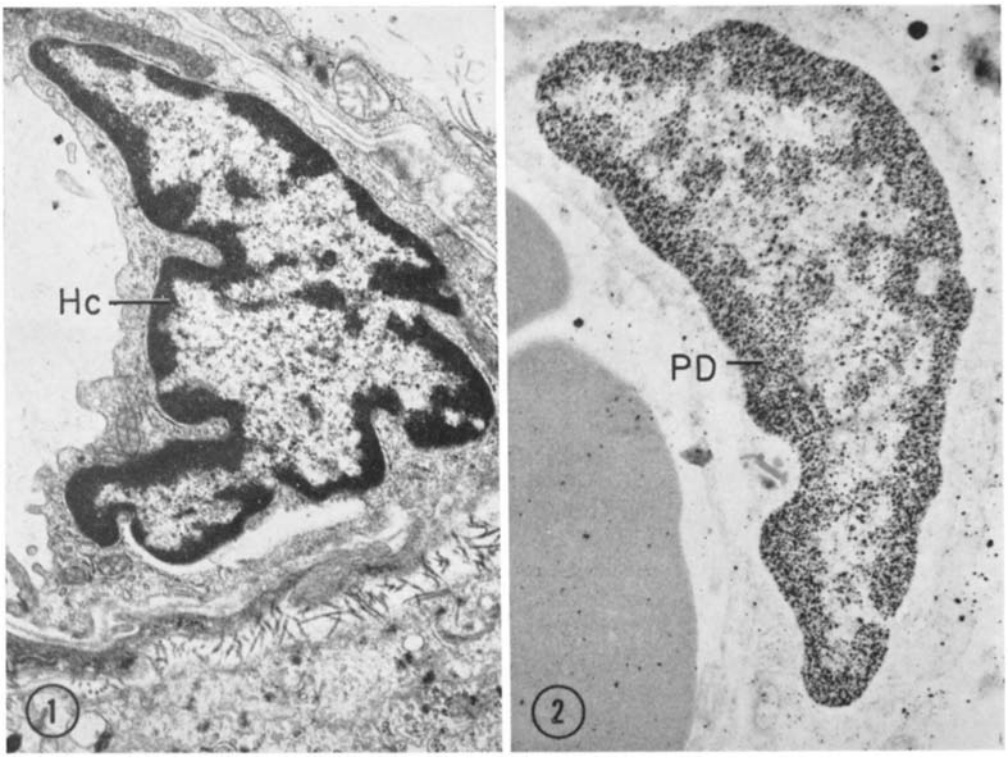

FIGURE 1 Heterochromatin (*Hc*) predominates at the nuclear margin of this endothelial cell. Glutaraldehyde and OsO_4 fixation. Uranyl acetate and lead citrate stained. × 11,000.

FIGURE 2 The distribution pattern of pyroantimonate deposits (*PD*) in the nucleus of this endothelial cell corresponds precisely with that of heterochromatin (see Fig. 1). Pyroantimonate-OsO_4 fixation. Unstained. × 16,000.

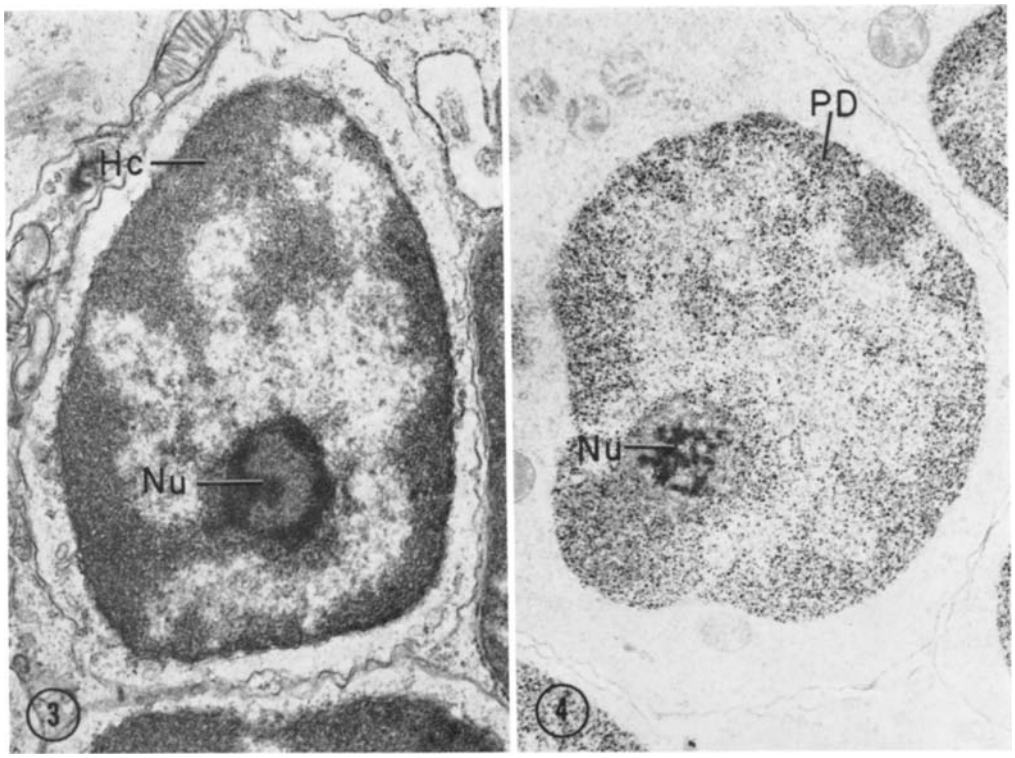

FIGURE 3 Heterochromatin (*Hc*) is located primarily at the margin of the nucleus and around the nucleolus (*Nu*) of this lymphocyte. Glutaraldehyde and OsO_4 fixation. Lead citrate stained. × 17,000.

FIGURE 4 Pyroantimonate deposits (*PD*) in this lymphocyte nucleus correspond in distribution with the heterochromatin (see Fig. 3). The electron opacity of the antimonate deposits in the nucleolus (*Nu*) differs from that of the deposits in the heterochromatin. The cytoplasm is devoid of deposits. Pyroantimonate-OsO_4 fixation. Unstained. × 18,000.

glutaraldehyde and osmium tetroxide possessed masses of heterochromatin which were distributed primarily at the nuclear margin.

The nuclei of these same cells fixed with the pyroantimonate-osmium tetroxide solution (Komnick's fluid) contained numerous electron-opaque deposits, most of which measured 20–40 mμ in diameter (Figs. 2, 4). These deposits, which presumably consist of sodium pyroantimonate, were evident in thin sections stained or unstained with heavy metals. The distribution of these deposits in the nuclei corresponded closely with that of heterochromatin visualized in the specimens fixed with glutaraldehyde and osmium tetroxide (see Figs. 1–4).

Nuclei with Sparse Heterochromatin

Compared with nuclei in the cell types described above, neuronal nuclei of rat trigeminal ganglia contained relatively little heterochromatin (Fig. 5). However, in specimens fixed sequentially with glutaraldehyde and osmium tetroxide and stained with uranyl acetate and lead citrate, a very narrow, irregular, intermittent rim of heterochromatin adhered to the nuclear envelope; and clumps of heterochromatin were attached to parts of the nucleolar surface. A few, small, ill-defined clumps, presumably composed of heterochromatin, were scattered free in the nucleoplasm.

Sections of neuronal nuclei of rat trigeminal ganglia fixed with Komnick's fluid showed pyroantimonate deposits with or without heavy metal staining (Fig. 6). Most of the deposits were located near the nuclear envelope, but others were congregated into a few small clumps which were free in the nucleoplasm or attached to the nucleolus. Thus, the pattern of distribution of these deposits closely resembled that of heterochromatin in nuclei

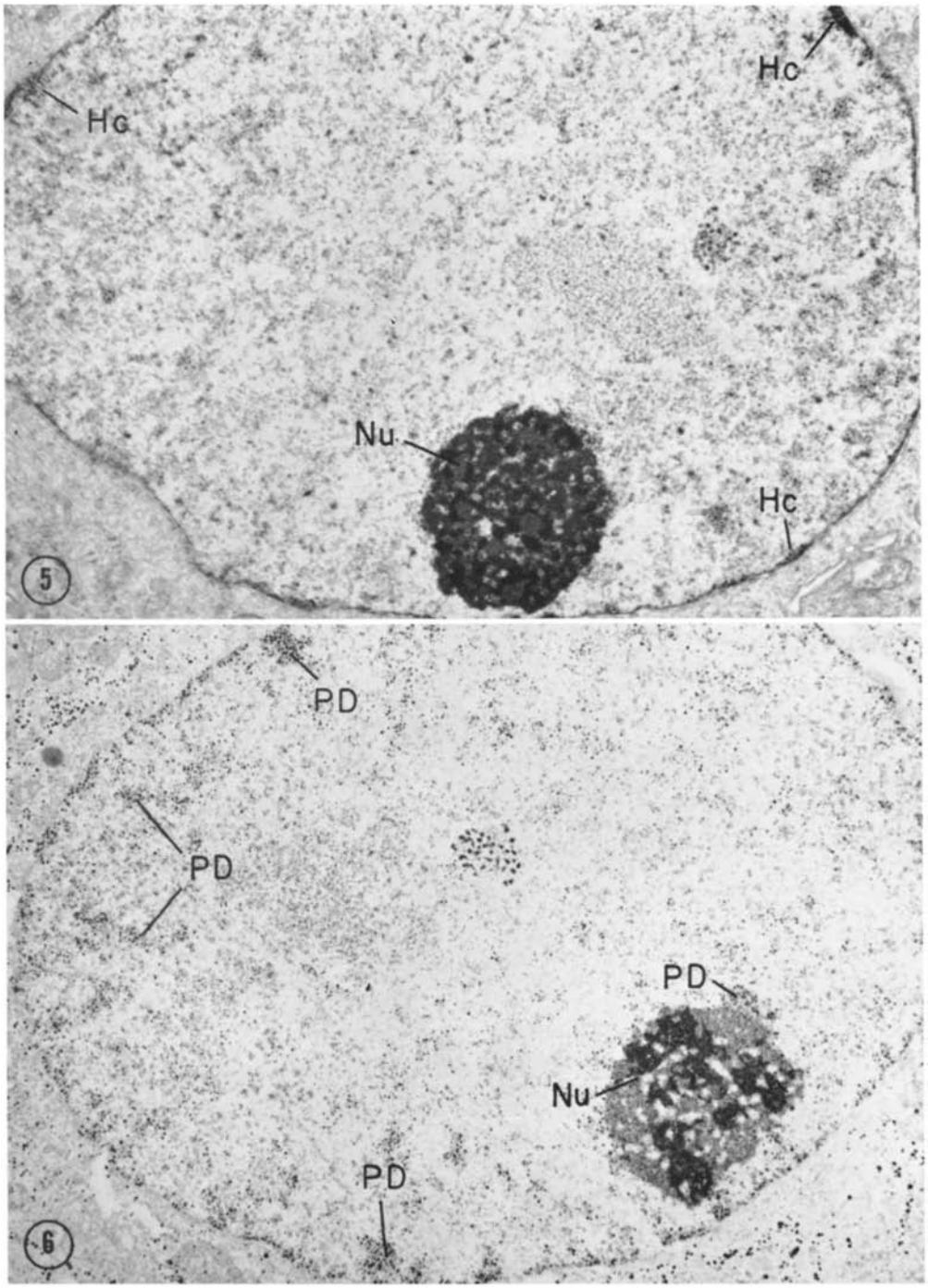

FIGURE 5 Heterochromatin (*Hc*) in this trigeminal neuronal nucleus is distributed in a thin intermittent rim near the nuclear envelope. Other small clumps of presumed heterochromatin are located free in the low density nucleoplasm. A prominent nucleolus (*Nu*) is located at the periphery of the nucleus. Glutaraldehyde and OsO_4 fixation. Uranyl acetate and lead citrate stained. × 9,000.

FIGURE 6 In this trigeminal neuronal nucleus, pyroantimonate deposits (*PD*) are localized in a narrow intermittent rim near the nuclear envelope and in clumps that are free in the nucleoplasm or attached to the nucleolus. The distribution of all these deposits closely resembles that of heterochromatin in specimens fixed and stained by routine methods (see Fig. 5). The antimonate deposits in the nucleolus (*Nu*) differ from those in the nucleoplasm. Pyroantimonate-OsO_4 fixation. × 9,000.

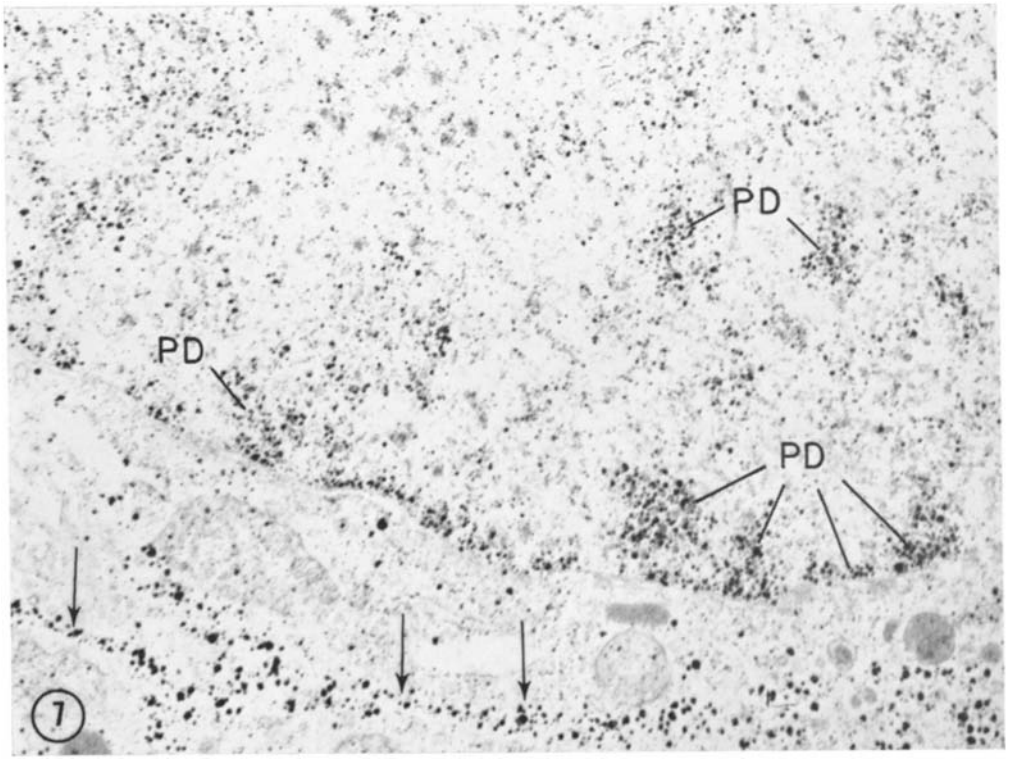

FIGURE 7 An enlargement of a portion of the nucleus shown in Fig. 6. At this high magnification it is evident that the clumps of pyroantimonate deposits (*PD*) are the only nuclear components with high electron opacity. Antimonate deposits located in the cytoplasm (arrows) may be associated with neurofilaments. Pyroantimonate-OsO_4 fixation. × 20,000.

of cells fixed with glutaraldehyde and osmium tetroxide (see Figs. 5 and 6). Antimonate deposits in the neuronal nuclei had the same diameter (20–40 mμ) as deposits in nuclei of endothelial, Schwann, and satellite cells and lymphocytes; this observation also suggests that the deposits in neuronal nuclei are located in regions of heterochromatin.

Nucleolar Deposits

In specimens fixed with the pyroantimonate-osmium tetroxide method, conspicuous deposits were observed in all nucleoli of the five cell types examined (e.g. Figs. 4 and 6). Indeed, three distinct types of intranucleolar deposits, differing in size and distribution, were evident. As will be reported in detail in a later paper, each type of antimonate deposit is localized in a particular nucleolar component visualized in specimens fixed and stained by routine methods.

Cytoplasmic Deposits

Except for the lymphocytes (Fig. 4), antimonate precipitates were not confined entirely to the nuclei in the cell types examined. The few deposits in the cytoplasm of endothelial, Schwann, and satellite cells appeared randomly distributed. Abundant antimonate precipitates in the cytoplasm of the trigeminal neurons, however, appeared to correspond in distribution with neurofilaments (Fig. 7). Moreover, in lead citrate–stained sections, antimonate deposits were aligned on neurofilaments in axons of trigeminal ganglia.

DISCUSSION

The present study demonstrates that tissue fixation with Komnick's potassium pyroantimonate-osmium tetroxide solution yields electron-opaque deposits that are localized in nuclear heterochromatin of endothelial, Schwann, satellite, and

neuronal cells of rat trigeminal ganglia and in lymphocytes of mouse cervical lymph nodes. This finding is not restricted to these few cell types, since similar nuclear deposits have been invariably encountered in a wide variety of tissues studied in this laboratory. In addition, nuclear deposits have been illustrated in cells of human sweat gland (2), rat neural tissues (4), and salt-secreting gland of the sea gull (9).

Antimonate deposits also have been localized in cytoplasmic structures of certain cells, including the sarcoplasmic reticulum and the T system of skeletal muscle (11, 12) and plasma membranes (2, 6, 7, 9) and mitochondria (2, 9) of cells specializing in electrolyte transport. Antimonate deposits also have been observed in synaptic vesicles (10).

The cation reacting with pyroantimonate anion to form the electron-opaque deposits is sodium, according to Komnick (8, 9) who found deposits in sodium-impregnated gelatin and in sodium-rich cells of the salt-secreting gland of the Herring gull. Evidence in support of this view was also provided by electron diffraction patterns which indicated presence of sodium antimonate in tissue fixed with Komnick's fluid (4). Further indication that the deposits may be sodium derives from the localization of antimonate deposits on the inner aspect of endothelial cell plasma membranes. The deposits are localized then on the opposite side of the plasma membrane from the sodium-potassium–activated ATPase (6).

The nuclear deposits could be interpreted on the basis of precipitation of the pyroantimonate anion with Na^+ cations salt linked to nucleic acid. Precipitation as sodium pyroantimonate would be consistent with the radioautographic evidence (1) for a high Na^+ concentration in nuclei. However, the antimonate ion could precipitate with other cations or possibly with basic peptides or alkyl amines in this site.

SUMMARY

Nuclei of several cell types in rat trigeminal ganglia and mouse cervical lymph nodes fixed in Komnick's solution of potassium pyroantimonate and osmium tetroxide contained prominent electron-opaque deposits that supposedly localize endogenous tissue sodium. On the basis of the distribution pattern of these deposits, they are localized in regions of heterochromatin. Other deposits, differing in size and compactness, were observed in nucleoli of these cells.

This work was supported by National Institutes of Health grants AM-10956 and AM-11028.

Received for publication 13 May 1968, and in revised form 18 June 1968.

BIBLIOGRAPHY

1. ALLFREY, V. G., R. MEUDT, J. W. HOPKINS, and A. E. MIRSKY. 1961. Sodium-dependent "transport" reactions in the cell nucleus and their role in protein and nucleic acid synthesis. *Proc. Natl. Acad. Sci. U.S.* **47**:907.
2. GRAND, R. J., and S. S. SPICER. 1967. Preliminary studies on the electron microscopic localization of sites of sodium transport in the human eccrine sweat gland. *Mod. Probl. Pediat.* **10**:100.
3. HARDIN, J. H., S. S. SPICER, and W. B. GREENE. 1967. Nucleolar ultrastructure clarified by pyroantimonate-osmium fixation. *J. Cell Biol.* **35**:54A.
4. HARTMANN, J. F. 1966. High sodium content of cortical astrocytes. *Arch. Neurol.* **14**:633.
5. ITOH, S., and I. L. SCHWARTZ. 1957. Sodium and potassium distribution in isolated thymus nuclei. *Am. J. Physiol.* **188**:490.
6. KAYE, G. I., J. D. COLE, and A. DONN. 1965. Electron microscopy: Sodium localization in normal and ouabain-treated transporting cells. *Science.* **150**:1167.
7. KAYE, G. I., H. O. WHEELER, R. T. WHITLOCK, and N. LANE. 1966. Fluid transport in the rabbit gallbladder. *J. Cell Biol.* **30**:237.
8. KOMNICK, H. 1962. Elektronenmikroscopie Lokalisation von Na^+ and Cl^- in Zellen und Geweben. *Protoplasma.* **55**:414.
9. KOMNICK, H., and U. KOMNICK. 1963. Elektronenmikroscopie Untersuchungen zur funktionellen Morphologie des Ionentransportes in der Salzdruse von Larus argentatus. *Z. Zellforsch. Mikroskop. Anat.* **60**:163.
10. SIEGESMUND, K. A., and H. F. EDELHAUSER. 1968. Sodium localization in cerebellum. *Anat. Record.* **160**:517.
11. TICE, L. W., and A. G. ENGEL. 1966. The localization of sodium pyroantimonate in frog muscle fibers. *J. Cell Biol.* **31**:118A.
12. ZADUNAISKY, J. A. 1966. The location of sodium in the transverse tubules of skeletal muscle. *J. Cell Biol.* **31**:C11.